J. Ocean Univ. China (Oceanic and Coastal Sea Research)
https://doi.org/10.1007/s11802-023-5304-3
ISSN 1672-5182, 2023 22 (4): 949-960
http://www.ouc.edu.cn/xbywb/
E-mail:xbywb@ouc.edu.cn

Penetration Tests of Multi-Bucket Foundation in Sand for Offshore Wind Turbines

ZHANG Puyang[1), 2), *], QI Xin[2)], ZHANG Chao[2)], LE Conghuan[1), 2)], and DING Hongyan[1), 2)]

1) *State Key Laboratory of Hydraulic Engineering Simulation and Safety*, *Tianjin University*, *Tianjin* 300072, *China*
2) *School of Civil Engineering*, *Tianjin University*, *Tianjin* 300072, *China*

(Received December 17, 2021; revised April 23, 2022; accepted June 14, 2022)

Abstract Suction foundations are generally installed with negative pressures to overcome the resistance of soils and complete the penetration, but excessive negative pressures are also avoided to cause seepage damages. In this paper, the model test method was used to analyze the movement characteristics of multi-bucket foundations in the process of sinking in sand, and the common calculation methods of sinking resistances are verified. The critical negative pressure corresponding to the seepage failure of foundation was determined under the action of increasing negative pressure step by step and the characteristics of soil failure were studied. The calculation formula of critical suction in sand was verified in application, and according to the test results, the value of seepage coefficient was modified, which provides an example for the study of suction foundation in sand soils.

Key words multi-bucket foundation; penetration test; penetration resistance; critical suction; seepage failure

1 Introduction

The suction bucket is a new type of foundation used in the offshore wind turbine in recent years. The pressure difference inside and outside the bucket formed by the water pump is used as the driving force against the resistance at the skin and the tip of the bucket when the foundation is installed. Compared with the traditional foundation, the offshore construction time is shorter, the controllability in the construction and installation process is stronger, and the construction accuracy is higher (Wu *et al*., 2018; Ding *et al*., 2020b; Shi *et al*., 2022; Zhang *et al*., 2022; Zou *et al*., 2022). Common suction foundations include composite bucket foundation and multi-bucket foundations. With its internal honeycomb sub-cabin structure, the composite bucket foundation can realize self-floating towing and accurate sinking and leveling (Ding *et al*., 2020a). Multi-bucket foundations mostly use jackets as the substructures, which has high structural rigidity and is more applicable to sea areas with a water depth greater than 30 m (Shonberg *et al*., 2017). The vertical driving force of the suction foundation sinking installation is composed of the self-weight and the pressure difference formed inside and outside the bucket. The sinking resistance is composed of the skin friction and the end resistance (Ding *et al*., 2017; Jia *et al*., 2018; Wang *et al*., 2019; Xiao *et al*., 2019) , as shown in Fig.1.

When the negative pressure of the bucket foundation is small, the cylindrical foundation cannot penetrate into the soil. When the negative pressure is large, a soil plug may be formed during the installation (Kim and Kim, 2019). When the negative pressure is too large, it may cause the soil seepage damage (Hu *et al*., 2018; Wu *et al*., 2020; Lin *et al*., 2021), making the bucket foundation fail to sink further, that is, installation failure. Therefore, the accurate prediction of the sinking resistance during the installation of the bucket foundation and the application of a reasonable negative pressure value based on the sinking resistance are the key to ensuring the successful foundation installation. For the penetration of mono-bucket, some scholars have proposed the usual calculation methods of the suction type foundation penetration resistance in sand (Houlsby and Byrne, 2005; Senders and Randolph, 2009), and the bearing capacity model and cone penetration test (CPT) model have been verified by experiments (Andersen *et al*., 2008).

However, the sinking and penetration of multi-bucket foundations in engineering require not only to correctly evaluate the sinking resistance, but also to control the inclination of the foundation during the installation process (Sahota and Wilson, 1982; Villalobos *et al*., 2010; Barari and Ibsen, 2012; Achmus *et al*., 2013). Det Norske Veritas (2017) put forward the requirement for the levelness of the offshore wind turbine foundation: the inclination angle is not more than ±5° after the installation is completed (Det Norske Veritas, 2017). Excessive inclination of the bucket during installation will increase the sinking resistance, because the negative pressure driving force must overcome the passive earth pressure caused by the inclination while overcoming the side friction and end resis-

* Corresponding author. E-mail: zpy_td@163.com

tance. And the greater the inclination and the buried depth are, the greater the negative pressure driving force is consumed to overcome the passive earth pressure, and the more difficult the leveling is.

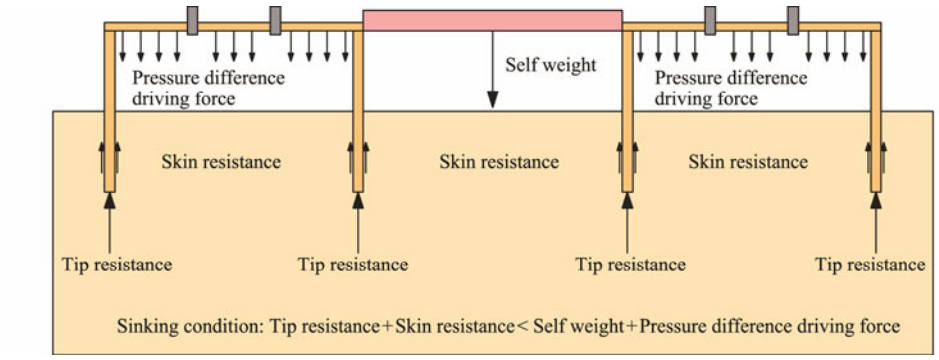

Fig.1 Penetration force conditions of multi-bucket foundations.

In this paper, the control method for the upper and lower limits of negative pressures was used to study the resistance and movement characteristics of the four-bucket foundation during the penetrating process. The critical negative pressure values and the seepage failure characteristics of four tube foundation under the action of increasing negative pressure step by step were studied by adopting the progressive negative pressure loading system. This article validates the existing equations for the penetration resistance and critical resistance through small scale model tests, ignoring the impact of seepage from multi-bucket foundations. The results of this study can be verified against the numerical simulation software, which is beneficial to the application of numerical simulation results to large size projects and provide guidance to practical projects.

2 Penetration Theory

2.1 Penetration Resistance

The penetration resistance of bucket foundation is closely related to the soil properties. Under the negative pressure, the water in the soil will flow in the soil pores, forming the seepage force, which will affect the penetration resistance. In the process of negative pressure penetration of tubular foundation in sandy soil, the seepage plays an important role in reducing resistances. The penetration resistance prediction model of bucket foundations in sand can be divided into two parts: One is the penetration resistance calculation model without considering the seepage effect, including the penetration resistance calculation model based on API specification (American Petroleum Institute, 2014) and DNV specification (Det Norske Veritas, 2017); The other part is the calculation model considering the effect of drag reduction, which are from the works of Houlsby and Byrne (2005) and Senders and Randolph (2009) respectively. The following four kinds of penetration resistance calculation models are described in detail.

1) Calculation model of penetration resistance based on API specification

$$f_{s,av} = 0.5K\gamma' z\tan\delta\,, \tag{1}$$

$$q_{\text{tip}} = 0.5\gamma' tN_r + qN_q\,, \tag{2}$$

$$N_q = \mathrm{e}^{\pi\tan\varphi}\tan^2(45+\frac{\varphi}{2})\,, \tag{3}$$

$$N_r = 1.5(N_q - 1)\tan\varphi\,. \tag{4}$$

Here, $f_{s,av}$ is the average value of the lateral friction resistance; z is the penetration depth, γ' is the effective weight of the soil; q_{tip} is the end resistance; Both N_q and N_r are end resistance calculation coefficients; t is the thickness of bucket, q is the effective unit weight of overlying soil; K is the ratio of horizontal and vertical effective stress of soil; δ is the friction angle between soil and bucket wall; φ is the internal friction angle of soil.

2) Calculation model of penetration resistance based on DNV specification

When calculating the penetration resistance of bucket foundation, the DNV code gives the calculation model of steel skirt without considering seepage effect based on CPT test:

$$Q_{\text{tot}} = k_p A_{\text{tip}} q_c(h) + A_{\text{wall}}\int_0^h k_f q_c(z)\mathrm{d}z\,. \tag{5}$$

Here, k_p and k_f are the coefficients of end resistance and side friction resistance respectively; $q_c(h)$ and $q_c(z)$ are end resistance and side friction resistance measured by the CPT test.

3) Penetration resistance calculation model of Houlsby and Byrne

Considering the influence of seepage on the effective stress of soil, Houlsby and Byrne (2005) proposed a calculation model on the penetration resistance of bucket foundation.

$$Q_{\text{tot}} = \int_0^h \sigma'_{vo}\mathrm{d}_z(K\tan\delta)_0(\pi D_0) + \int_0^h \sigma'_{vi}\mathrm{d}_z(K\tan\delta)_i(\pi D_i) + \sigma'_{\text{end}}(\pi D_t)\,, \tag{6}$$

$$\sigma'_{vo} = (\gamma' + as/h)Z_0[\exp(h/Z_0) - 1]\,, \tag{7}$$

$$\sigma'_{vi} = (\gamma' - (1-a)s/h)Z_i[\exp(h/Z_i) - 1]\,, \tag{8}$$

$$\sigma'_{\text{end}} = \sigma'_{vo} N_q + \gamma'(t - 2x^2/t) N_\gamma . \quad (9)$$

Here, t is the thickness of bucket; as is the excess pore water pressure; $as/\gamma_w h$, $(1-a)s/\gamma_w h$, are the average downward and upward hydraulic gradients respectively; a, Z_0, and Z_i are the coefficients.

4) Penetration resistance calculation model of Senders and Randolph

Based on the DNV method, assuming that the influence of seepage on the end and interior resistance of bucket foundation is linear, while the influence of seepage on the external wall resistance of bucket foundation can be ignored, Senders and Randolph (2009) proposed a calculation model of the penetration resistance in sand :

$$Q_{\text{tot}} = A_{so}\int_0^h k_f q_c(z)\mathrm{d}_z + \left[A_{si}\int_0^h k_f q_c(z)\mathrm{d}_z + k_p A_{\text{tip}} q_c(h)\right] \cdot\left(1 - p/p_{\text{crit}}\right), \quad (10)$$

where A_{so} is the area within the penetration depth of the outer wall of the bucket foundation; A_{si} is the area within the penetration depth of the inner wall of the bucket foundation; p is the applied suction value; p_{crit} is the critical suction value of bucket foundation.

2.2 Critical Suction

The pressure value of the bucket foundation in the case of seepage failure is the critical negative pressure of the suction foundation during the installation. The results show that the seepage failure of the bucket foundation during the process of negative pressure sinking usually occurs at the hydraulic outlet. Critical hydraulic gradient appears first at the position of the bucket end with large hydraulic gradient during the process of negative pressure installation of the bucket foundation. However, the seepage failure is not easy to occur at the end position due to the constraint of the surrounding soil on the end soil mass (Hu *et al*., 2018). In the researches on the critical suction of bucket foundation under the negative pressure penetration, many scholars have given the calculation model of critical negative pressure value corresponding to the failure of foundation soil. Among them, the typical models are shown as follows.

1) Feld model

Feld (2001) used the numerical software SEEP, combined with CPT method, to consider the influence of effective stress degradation caused by suction, and put forward the calculation formula of critical suction.

$$\frac{p_{cr}}{\gamma' D} = 1.32\left(\frac{h}{D}\right)^{0.75} . \quad (11)$$

Here, p_{cr} is the critical negative pressure; γ' is the effective unit weight of foundation soil; h is the penetration depth of foundation; D is the bucket diameter.

2) Houlsby and Byrne model

Houlsby and Byrne (2005) considered the difference of soil permeability coefficients inside and outside the bucket, and took the average hydraulic gradient within the foundation penetration depth as the standard to measure the seepage failure, through finite element simulation, established the calculation formula of critical suction:

$$\frac{p_{cr}}{\gamma' D} = \left(\frac{h}{D}\right)\left(1 + \frac{\alpha_1 k_{fac}}{1-\alpha_1}\right), \quad (12)$$

$$\alpha_1 = 0.45 - 0.36(1 - \mathrm{e}^{-0.28h/D}) . \quad (13)$$

Here, k_{fac} is the ratio of the permeability coefficient inside to outside the bucket; α_1 is the coefficient related to h and D.

3) Senders and Randolph model

Senders and Randolph (2009) assumed that the increase of suction caused the linear changes in the internal friction resistance of the bucket wall and the resistance at the skirt end, that is, the excess pore water pressure of the soil caused by suction changes linearly, while the soil outside the bucket is not affected by the penetration suction. Through the finite element software PLAXIS, the critical suction calculation formula is derived:

$$\frac{p_{cr}}{\gamma' D} = \left\{\pi - \arctan\left[5\left(\frac{h}{D}\right)^{0.85}\right]\left(2 - \frac{2}{\pi}\right)\right\}\left(\frac{h}{D}\right). \quad (14)$$

4) Ibsen and Thilsted model

Ibsen and Thilsted (2011) used finite difference program FLAC3D to calculate the seepage path at the maximum hydraulic gradient (*i.e*., the outlet of the top cover) in uniform sand, and compared with previous studies (Senders and Randolph, Feld, Houlsby), improved the critical suction calculation formula as follows:

$$\frac{p_{cr}}{\gamma' D} = \left\{2.86 - \arctan\left[4.1\left(\frac{h}{D}\right)^{0.85}\right]\left(\frac{\pi}{2.62}\right)\right\}\left(\frac{h}{D}\right). \quad (15)$$

3 Model Test in Sand

3.1 Test Model and Device

In experiment, a four-bucket model is used. The overall model consists of three parts: the bucket, the jacket and the wind turbine tower. The photo of overall model is shown in Fig.2a. Considering the research content of this paper, we take the four-bucket foundation as the experimental object, as shown in Fig.2b, and the model size parameters are shown in Fig.2c and Table 1.

The four-bucket model was made of steel, and the buckets are rigidly connected by channel steel. An air valve is installed on the top of the bucket, which can be used to pump air or water out and measure the pressure, As shown in Fig.2c. The suction hole is connected with the suction vacuum pump, and the vacuum pump works to extract the gas in the bucket to form a negative pressure in the bucket, and carry out the four-bucket foundation sinking and leveling; the measuring hole is connected with the negative pressure sensor to monitor the pressure changes in real time in the bucket during the sinking and leveling process.

The four-bucket foundation negative pressure sinking and leveling test device is shown in Fig.3a The penetra-

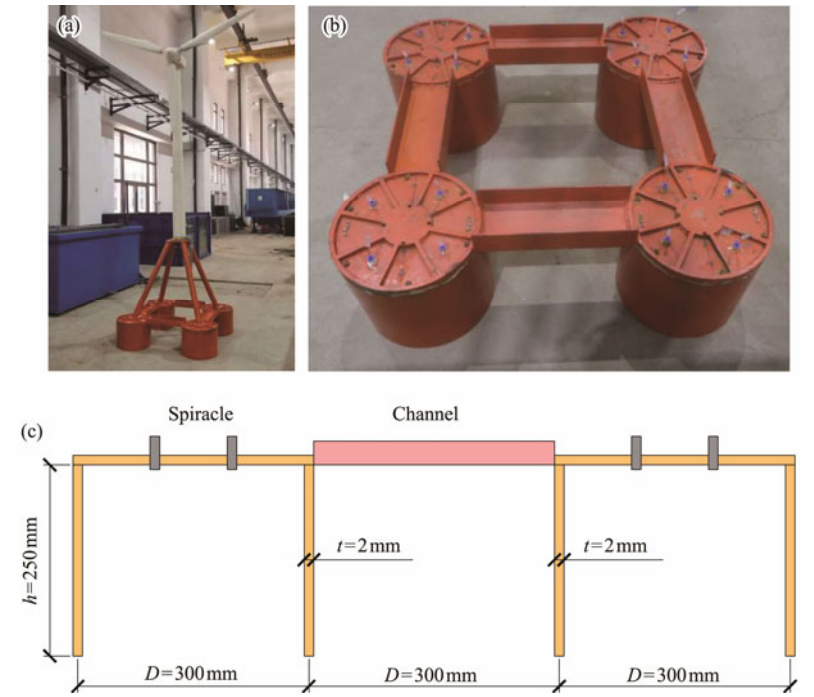

Fig.2 Test model. (a), overall model; (b), four-bucket model; (c), model size parameters.

Table 1 Model parameter

Diameter (mm)	Height (mm)	Thickness (mm)	Bucket distance (mm)	Mass (kg)
300	250	2	300	55

tion and leveling dynamic system provides the driving force for the experiment , in which the vacuum pump provides negative pressure. Between the vacuum pump and the foundation, the vacuum saturation cylinder provides a stable negative pressure for the four-bucket foundation. The inclinometer is arranged between the bucket foundations to detect the inclination of the four-tube foundation during the sinking and leveling process. The laser displacement sensor was arranged directly above the cylindrical foundation to monitor the negative pressure penetration depth of the cylindrical foundation in real time.

3.2 Soil Parameters in Experiment

The length × width × height of the test soil box was 2 m × 2 m × 1.5 m, as shown in Fig.3b. The sand was evenly layered into the model box, and the thickness of each layer was no more than 0.2 m, and water is added for one month to fully saturate the sand. It is necessary to maintain the consistence of test sand under the different test conditions. Water was injected from the drain value until the water surface reaches 10 cm above the soil surface, and then the method of drainage from the lower part was used to accelerate the saturated compaction of the sand. The next test was carried out after standing for 24 h, so as to ensure that the soil properties of each test are the same. A 1 cm deep water layer was reserved on each group of test soil surface to ensure that the soil was in saturated state during the test.

The soil parameters are measured through a series of geotechnical tests. The results of direct shear test and screening test are shown in Figs.4a and b respectively, and the soil parameters are listed in Table 2. The shear test was carried out at a shear speed of 0.8 mm min^{-1}, ensuring that the sample sand was broken within 3–5 min. Screening tests were carried out with fine sieves of 2 mm, 1 mm, 0.5 mm, 0.25 mm, 0.1 mm and 0.075 mm, and the percentage of each particle group in the sand sample was obtained. According to the sand classification criteria, the test sand was fine sand.

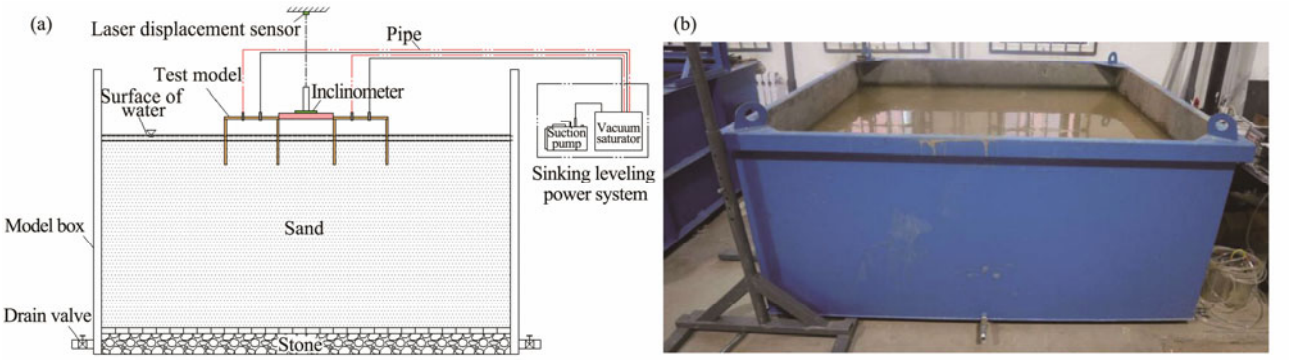

Fig.3 Test device. (a), sinking and leveling test device; (b), soil box.

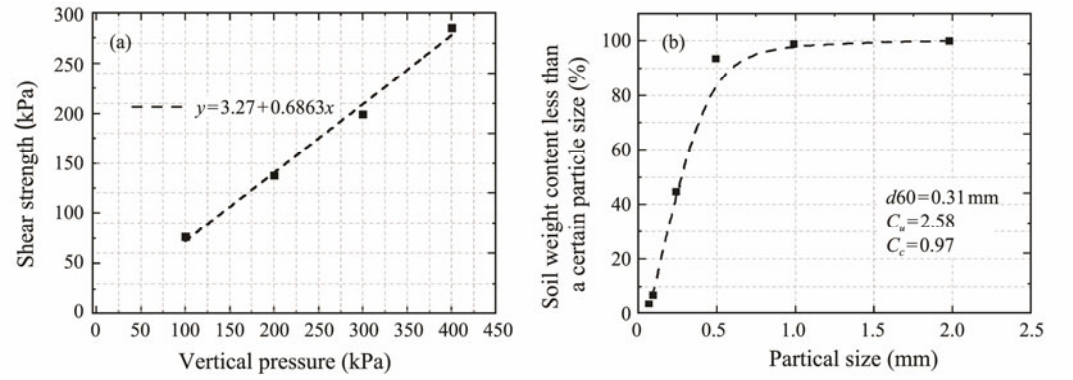

Fig.4 Geotechnical test results. (a), direct shear test; (b), screening test.

Table 2 Geotechnical properties of the test soil

Item	Properties
Saturated density (g cm^{-3})	2.2
Water content (%)	22.41
Internal friction angle (˚)	34.46
Cohesion (kPa)	3.27
Void ratio	0.57
Compression modulus (MPa)	18
Relative density	0.69
Non-uniformity coefficient	2.58
Curvature coefficient	0.97
$d60$ / $d30$ / $d10$ (mm)	0.31 / 0.19 / 0.12

4 Study on Penetration Conditions of Multi-Bucket Foundation in Sand

The reasonable application of negative pressure was an important part in the research of bucket foundation installation. The reasonable control of negative pressure during the installation process can reduce the probability of excessive inclination, so as to improve the installation speed. Based on the API resistance calculation model and Feld critical negative pressure calculation model of bucket foundation during the sinking, the working conditions listed in Table 3 were adopted in this study. The different initial negative pressures were set, and then the negative pressure was increased by 1 kPa per stage.

Table 3 Test conditions

Test number	Initial negative pressure (kPa)
PS-1	1
PS-1.5	1.5
PS-2	2

The penetration process of bucket foundations consists of two stages:

First, we check whether the inclination angle of the foundation after its self-weight installation was less than 0.25˚. If the inclination angle of the foundation meets the installation requirements of negative pressure sinking, the negative pressure loading will be carried out; otherwise, the bucket foundation will be leveled. The final sinking depth under the action of foundation self-weight will be recorded.

In the second stage, the vacuum pump was used to load the foundation step by step. During the negative pressure loading process, the air inside the storage negative pressure device was pumped first. After the negative pressure reaches the specified level, the air valve between the negative pressure device and the bucket foundation was opened to load the foundation under the negative pressure. During the loading process, the inclination angle of the bucket foundation was detected by the inclinometer, and the air valve of each bucket on the multi-bucket foundation was controlled to keep the inclination angle within 0.25˚. After the foundation negative pressure penetration is stable, the next negative pressure loading condition is applied until the foundation was installed in place.

4.1 Inclination Angle in the Process of Multi-Bucket Foundation Penetration

In the negative pressure control plan of four-bucket foundation sinking, the theoretical critical negative pressure of the bucket was used as the upper limit of negative pressure to avoid the penetration damage; the lower limit of negative pressure was designed based on the API specification to ensure that the foundation can be sunk. The foundation sinking negative pressures were compared with the theoretical negative pressure control values, as shown in Fig.5. The negative pressures of the tests fell between the upper and lower limits of the negative pressure.

During the sinking of the foundation, the inclination angle was adjusted within the range of ±0.25˚, which meets the requirements of the bucket foundation sinking process specification. Taking the PS-1 penetrating test as an example, the inclination angle control during the sinking and penetrating process of the foundation was explained. In the PS-1 penetrating test, the internal negative pressure and the inclination angle of the foundation are shown in Figs. 6 and 7. The inclination angle of the foundation was controlled by adjusting the negative pressure inside the bucket. When the foundation was inclined, the low-elevation bucket negative pressure valve was closed and then opened until the inclination angle decreases to the required value. It is stipulated that the bucket B to A direction is the positive direction of the X axis, and the C to D direction is the positive direction of the Y axis. As shown in Fig.8, at 2500 s

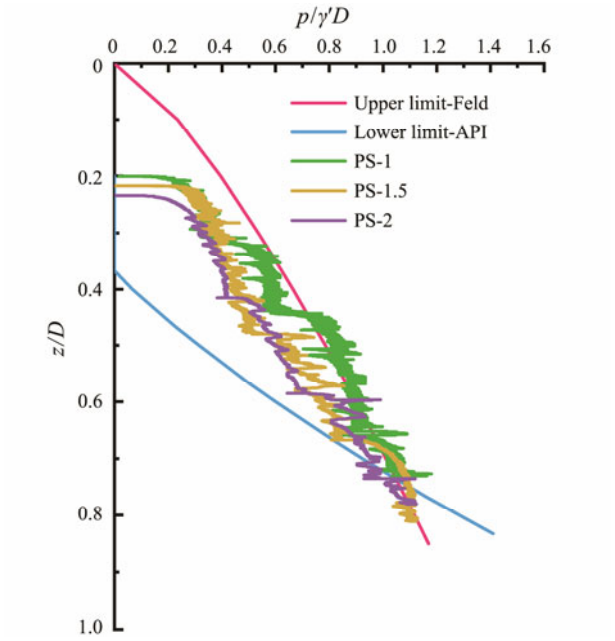

Fig.5 Dimensionless sinking negative pressure.

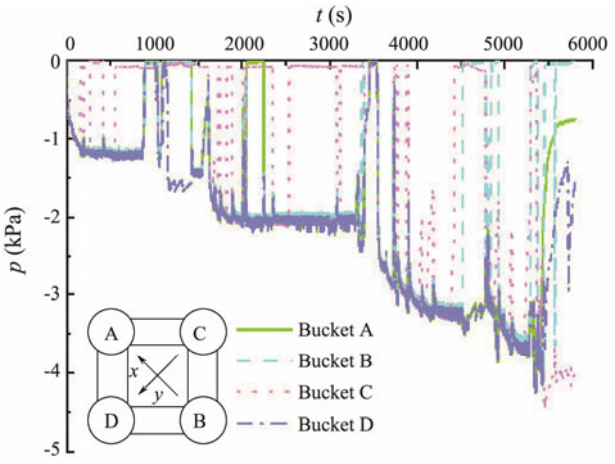

Fig.6 Variation of negative pressures in the buckets.

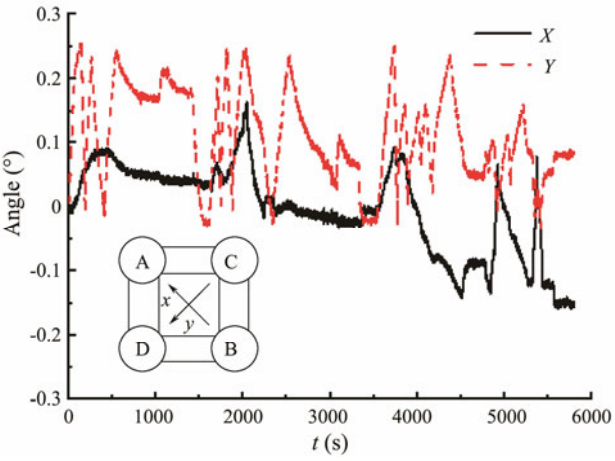

Fig.7 Variation of the inclination angles of foundation during its sinking process.

the inclination angle Y is positive, indicating that the bucket D is high. At this time, the negative pressure valve of the low bucket C was closed, as shown in Fig.6, and the negative pressure inside the bucket C was reduced to 0. Under the negative pressures in buckets A, B and D, the foundation was leveled and the inclination angle was reduced. At 3500 s, the inclination angle in the Y direction was reduced to 0, then the bucket C valve was opened, and the foundation continued to sink.

4.2 Multi-Bucket Foundation Sinking Resistance

In the penetrating test, the penetrating negative pressure is gradually increased by 1 kPa each time to the maximum of 4 kPa until the foundation installation is completed. The variation of loaded negative pressure and penetration depth are shown in Figs.8 and 9, respectively. The penetration depths of the foundations under different negative pressures for each working condition are shown in Table 4. During the sinking process of the four-bucket foundation, the displacement-time curve is steep at the initial time that each penetrating negative pressure is loaded, and the foundation sinks at a greater rate. As the sinking depth increases, the penetration resistance increases, and the slope of the displacement curve also becomes smaller until the four-bucket foundation is balanced under the sinking negative pressure.

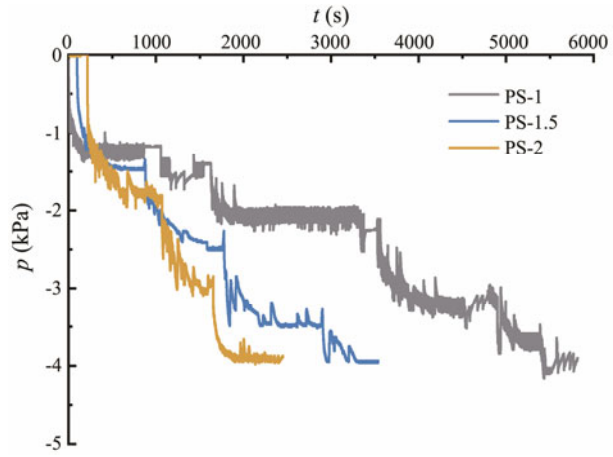

Fig.8 Loaded negative pressures in sinking tests.

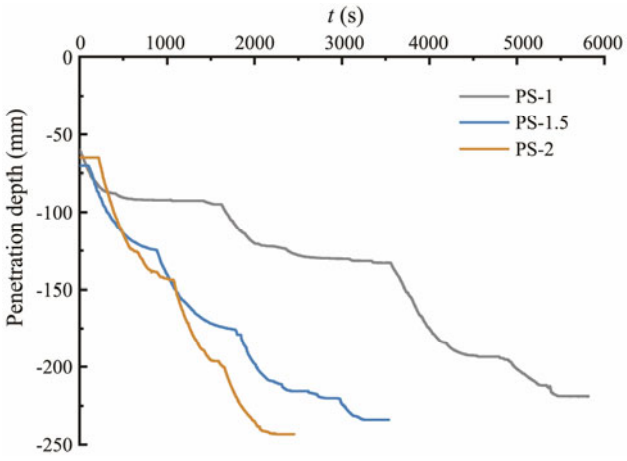

Fig.9 Foundation displacements in sinking tests.

According to the penetrating displacement curve, the pe-

netrating velocity of the foundation under different initial negative pressures can be obtained. In the test PS-1, the initial negative pressure is 1 kPa, the foundation takes about 500 s to sink 32 mm, with the average settlement speed of 0.064 mm s^{-1}. The test PS-1.5 is carried out at the initial negative pressure of 1.5 kPa, the foundation displacement is 54 mm, which takes about 700 s, and the average settlement velocity is 0.076 mm s^{-1}. The foundation in the test PS-2 under the initial negative pressure of 1.8 kPa has the settlement displacement of 79 mm in 750 s and the average settlement velocity is 0.105 mm s^{-1}. The settling depths of foundation in test PS-1.5 and PS-2 are greater than that of PS-1, but the average settling speeds are increased by 18.8% and 64%. If the same settling depth is used to measure the penetrating speed under negative pressures, the large penetrating negative pressure may help to complete the installation more quickly.

Therefore, during the negative pressure penetrating process of the bucket foundation, a suitable negative pressure can keep the penetrating speed of the foundation at a higher value, thereby improving the efficiency and shortening the working time at sea.

Table 4 Test penetration depths corresponding to the different negative pressures

Test number	Negative pressure (kPa)	Displacement (mm)
PS-1	0	60
	1	92
	2	132
	3	193
	4	220
PS-1.5	0	70
	1.5	124
	2.5	172
	3.5	218
	4	221
PS-2	0	65
	2	144
	3	196
	4	243

In this paper, the sinking resistance of the four-bucket foundation was calculated based on the API specification. The theoretical sinking resistance value of four-bucket foundation at 250 mm is 1960 N. When the bucket foundation sinks, a soil plug will form inside the bucket, which will affect the follow-up installation of the foundation. Among the three sets of penetrating tests, the test PS-2 was less affected by the soil plug, and the inner top of the bucket sinks to the soil surface, so it can better reflect the final penetration characteristics of the four-bucket foundation.

The sinking resistance of the foundation at each level of sinking balance is equal to the sum of the foundation own weight and the driving force formed by the sinking negative pressure. At the last stage of the test PS-2, the sinking negative pressure was 4 kPa, and the sinking resistance was 1680 N according to the foundation sinking balance principle. The difference of sinking resistance between the test and API estimation is 14%. The tests PS-1 and PS-1.5 are greatly affected by the soil plugs in the buckets, and the penetrating resistances when the settlement is stable at 193 mm and 218 mm are compared with the theory values respectively. The penetrating resistances derived from the tests according to the balance equation are 1403 N and 1445 N. Based on the API model, the resistances at the corresponding settlement depths are 1288 N and 1566 N. The differences between the theoretical and experimental values of the penetrating resistance are 8.2% and 7.7%. The comparison between the theoretical value and the experimental value of the penetration resistance is shown in Fig.10. The dimensionless test penetration resistance *vs*. depth curves are shown in Fig.11.

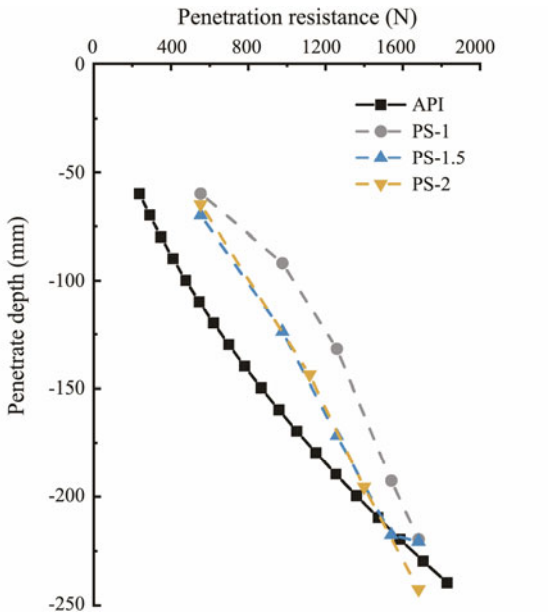

Fig.10 Curves of penetration resistance test values and theoretical values.

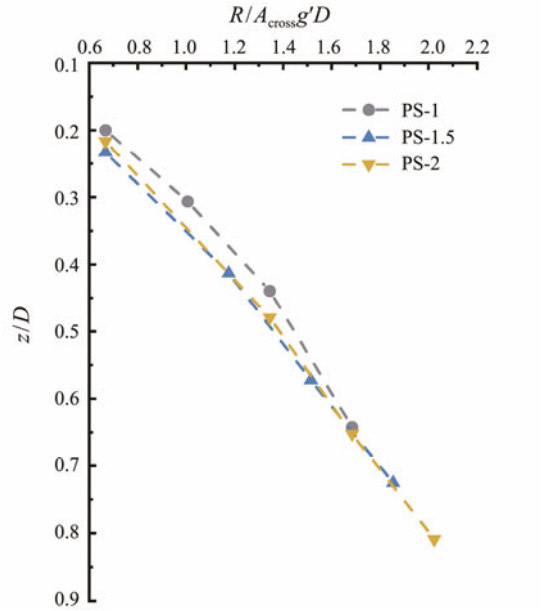

Fig.11 Dimensionless test penetration resistance *vs*. depth curves.

The penetration resistance of the four-bucket founda-

tion increases with the penetration depth, and the slope of the resistance curve has a steeper trend. For example, the slope of the relationship curve between the penetration resistance and the penetration depth in PS-1 test increased obviously with the depth, which is consistent with the development law of the penetration resistance for the bucket foundation. Taking the larger sinking negative pressure as the initial sinking negative pressure value, the speed at which the sinking resistance increases with the sinking depth can effectively be reduced during the sinking and penetration process. The test PS-1.5 and PS-2 use 1.5 kPa and 2 kPa as the initial settling negative pressure, and the test PS-1 uses 1kPa as the initial settling negative pressure. As shown in Fig.11, the slopes of the PS-1.5 and PS-2 curves are obviously lager than that of the PS-1 curve, indicating that the penetrating resistances of the test PS-1.5 and PS-2 increase more slowly due to the obvious reduction of the seepage drag effect under the action of large negative pressures.

5 Study on Critical Suction of Multi-Bucket Foundation in Sand

It could be found from the sinking tests that a larger initial negative pressure could reduce the sinking resistance, which was beneficial to the improvement of installation efficiency. However, there should be a certain limit to the maximum value of sinking negative pressures. Once the applied suction exceeds a certain limit, the sand in the foundation will be penetrated and damaged, and the internal sealing environment of the bucket will be destroyed. The bucket foundation cannot sink further under the action of driving negative pressures.

Ignoring the influence of the seepage field between the four-bucket foundation buckets, that is, the seepage field of each bucket of the four-bucket foundation is independent of each other, the critical negative pressure of any bucket is the overall critical negative pressure of the foundation.

Hoist the four-bucket foundation above the designated installation position, then install the laser displacement meter, pressure measurement and vacuum suction rubber pipes, as shown in Fig.12a. After the installation is completed, the inclinometer and hoisting equipment are used to level the foundation until the foundation is stationary. Slowly relax the sling, and wait when the foundation sinks by self-weight and stabilize at some level. Gradually increase the negative pressure to sink the foundations to the depth of 100 mm, 150 mm and 200 mm respectively, and the corresponding test number is listed in Table 5. Then restrict the vertical displacement of the foundation, and increase the negative pressure in the cylinder in a very short time, as shown in Fig.12b. Finally, the critical negative pressure value is determined when the foundation soil at the corresponding depth is damaged by seepage.

The critical negative pressures of the four-bucket foundation are calculated when the penetration depth is 100 mm, 150 mm and 200 mm. The influence of seepage under negative pressure is not considered in the Feld model, Senders and Randolph model and Ibsen and Thilsted model, but involved in the Houlsby and Byrne model by introducing the ratio of permeability coefficients inside and outside the bucket, set as 2, 2.5 and 3 respectively in this paper. The calculation results are shown in Figs.13 and 14.

Table 5 Critical negative pressure test conditions

Test number	Initial negative pressure (kPa)
T100-1	2
T100-2	3
T100-3	1.5
T150-1	3
T150-2	3
T150-3	2
T200	3

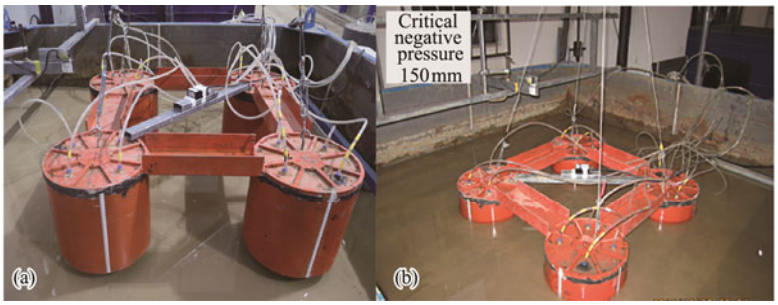

Fig.12 Critical negative pressure tests. (a), leveling before installation; (b), sinking to the specified depth.

5.1 Experimental Phenomena in the Critical Negative Pressure Tests

Taking the critical negative pressure test T100 as an example, the permeation failure process of foundation soils is explained. When the applied negative pressure does not reach the critical value, the foundation soils may not be damaged, but some of soil around the tube was slightly sunken, as shown in Fig.15a; As the negative pressure level increases, cracks appear on the surface of the soil around the outer wall of the bucket, and the local depression of the soil near the tube wall increases, indicating that the critical negative pressure value of the four-bucket foundation is about to reach, and the penetration failure of foundation soils is about to occurs, as shown in Fig.15b; The negative pressure inside the bucket increases by one level again, and the seepage failure trend of the soil becomes more obvious. Finally, the soil outside the cylinder begins to flow into the

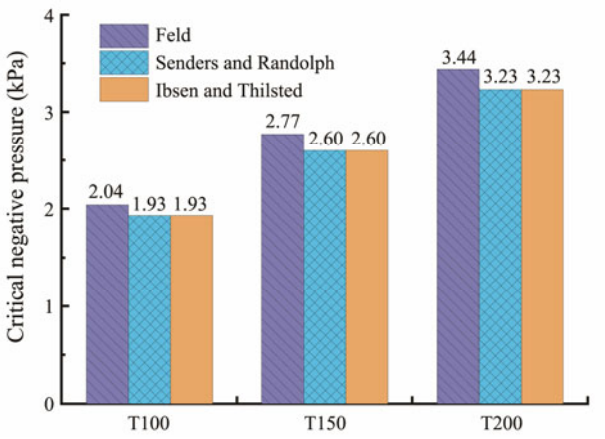

Fig.13 Critical negative pressures (permeability coefficient not considered).

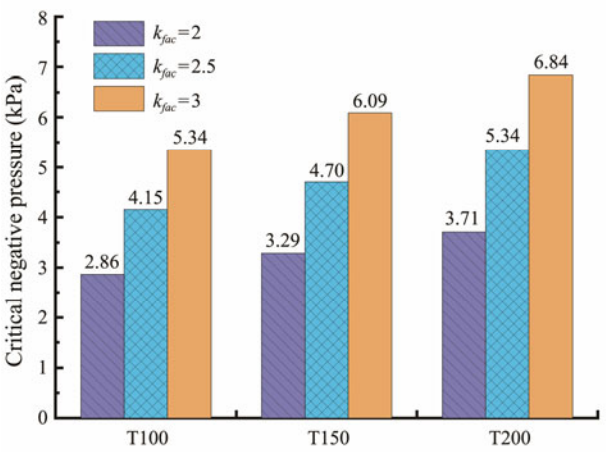

Fig.14 Critical negative pressures (considering permeability coefficient).

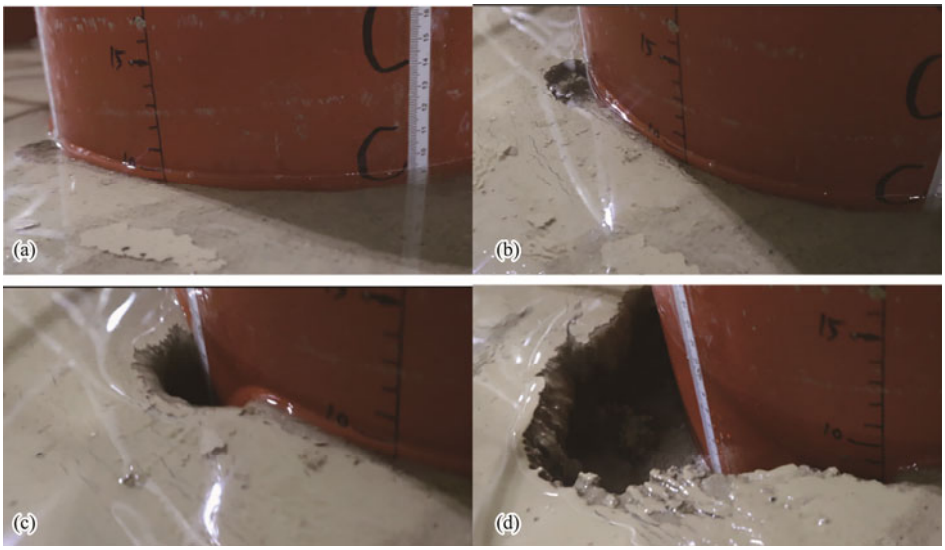

Fig.15 Seepage failure process of foundation soils. (a), before penetration failure; (b), impending osmotic damage; (c), penetration failure occurring; (d), final penetration failure.

cylinder along the seepage channel, and the seepage failure of foundation soils occurred, as shown in Fig.15c; Under the critical negative pressure, the soil outside the bucket continues to pour into the bucket until the channel was penetrated. At this time, the enclosed space inside the bucket was destroyed, and the internal and external pressure difference decreases rapidly through the seepage channel. The final seepage failure state of the foundation soil is shown in Fig.15d.

5.2 Results of Critical Negative Pressure Tests

When the penetration depth of the four-bucket foundation is 100 mm, the loading negative pressure in the test and the actual negative pressure in the bucket are shown in Figs.16 and 17 respectively. When the loading negative pressure level of the four-bucket foundation reaches the critical negative pressure value, the foundation soil is about to undergo the seepage failure. After this negative pressure inside the bucket continues to act for a period of time, the seepage failure occurs. The soil outside the foundation flows into the bucket, forming a sand piping channel, and the negative pressure inside the foundation decreases rapidly.

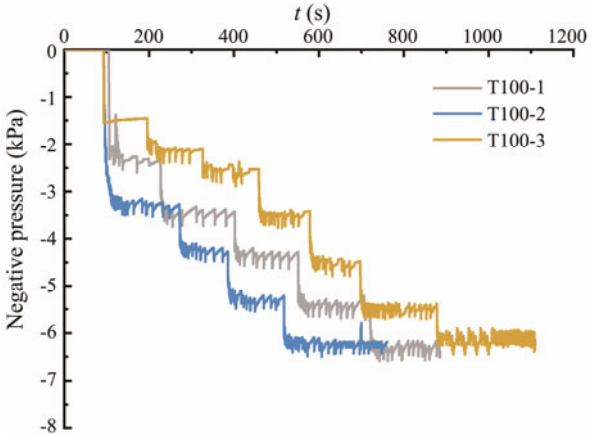

Fig.16 Loading negative pressures.

When the foundation is penetrated to 100 mm, the pressure values corresponding to the seepage failure are 6.3 kPa, 6.3 kPa and 6 kPa for the test T100-1, T100-2 and T100-3 respectively. The difference of critical values between dif-

ferent negative pressure application methods is no more than 5%. Therefore, the critical negative pressure value of four-bucket foundation model in our tests is 6kPa.

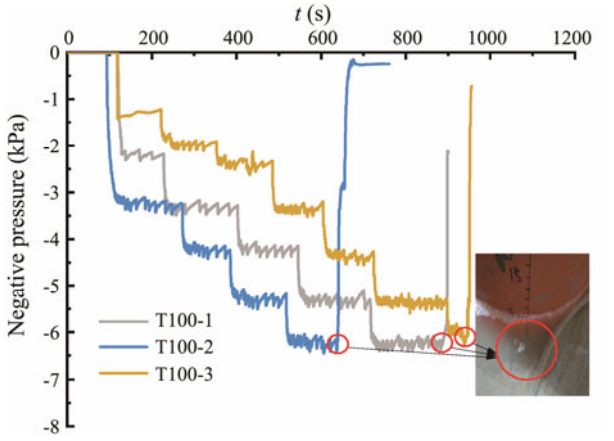

Fig.17 Negative pressures in the buckets.

When the penetration depth is 150 mm, the loading negative pressure, the negative pressure in the bucket, and the penetration failure morphology are shown in Figs.18 and 19. For the test T150-1, T150-2 and T150-3, the negative pressure in the bucket when the permeable failure occurs is 9.2 kPa, 9 kPa, and 8.6 kPa, respectively. Under the action of three different loading methods, the maximum difference in the critical negative pressure is 7%. Therefore, the critical negative pressure value corresponding to the penetration failure of the four-bucket foundation at a penetration depth of 150 mm is 9 kPa.

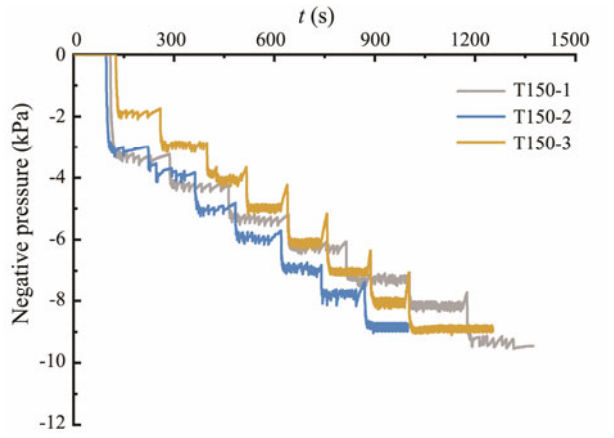

Fig.18 Loading negative pressures.

When the four-bucket foundation sinks to 200 mm, the loading negative pressure, the internal pressure of bucket and the seepage failure morphology are shown in Fig.20. The negative pressure inside the bucket drops sharply when the negative pressure is loaded to 10 kPa, and the seepage failure of the cylindrical foundation occurs.

For the calculation models without considering the influence of seepage coefficients on critical negative pressures, including the Feld model, Senders and Randolph model and Ibsen and Thilsted model, the change curves of dimensionless critical negative pressures with penetration depths, combined with the experimental results are shown in Fig.21, where S is critical negative pressures. The theoretical negative pressure calculated by the Feld model was slightly larger than the other two models. The negative pressures at the penetration depth of 1/3D, 1/2D and 2/3D are taken as the theoretical critical negative pressure values. After dimensionless disposal, the theoretical critical negative pressure was 0.575, 0.785 and 0.978, respectively. The dimensionless critical negative pressure values obtained from the tests at the penetration depths of 1/3D, 1/2D and 2/3D are 1.7, 2.5 and 2.8, which were 2.95 times, 3.18 times and 2.86 times of the theoretical critical negative pressures respectively. The critical negative pressure obtained from the tests was about 2 times higher than the theoretically calculated critical negative pressures. The theoretical values are used as the upper limits of negative pressure control when the penetrating is carried out during the construction for a high safety reserve.

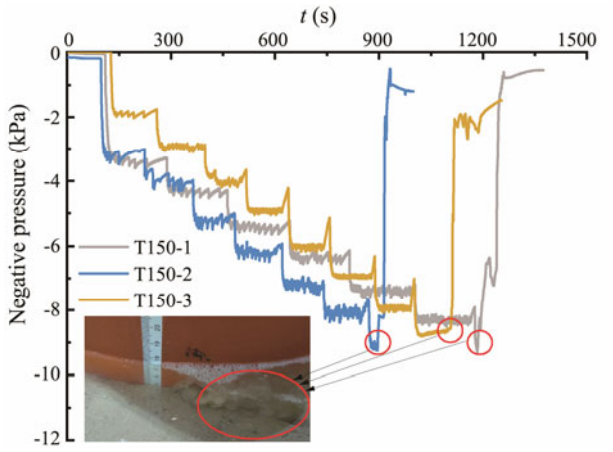

Fig.19 Negative pressures in the buckets.

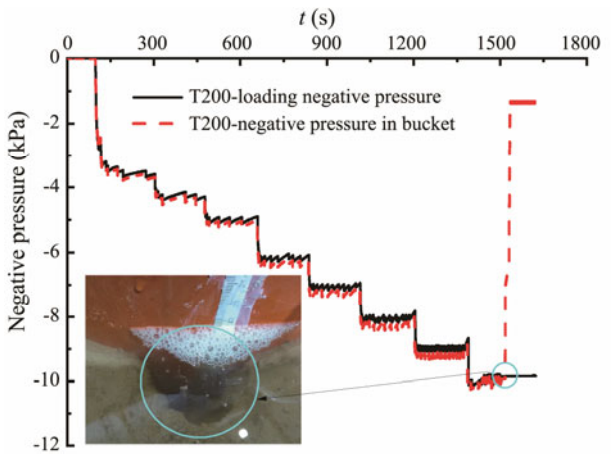

Fig.20 Negative pressures for the critical test T200.

The critical negative pressure values in the four-bucket foundation tests are much higher than the theoretical values calculated by the models above. It can be attributed to two points: One is that during the process of negative pressure penetration, the water seeps inside the soil body, and the pores in the soils become larger under the action of upward seepage force, resulting in the increase of per-

meability coefficient and the critical negative pressure that the soil can bear before seepage failures. The other is that the models do not consider the change of the permeability coefficient. The increase of the permeability coefficient can reduce the seepage gradient at the outlet of the sand in the bucket, causing the actual critical negative pressure to be larger than those calculated by the models.

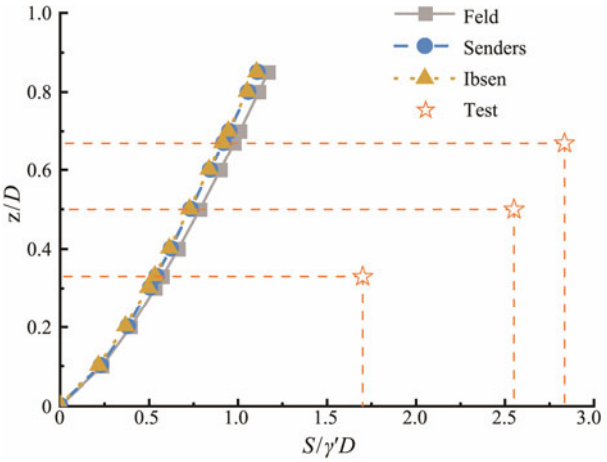

Fig.21 Theoretical and experimental negative pressures without considering the seepage effect.

Given that the soil inside the bucket would become loose under the action of negative pressure, Houlsby and Byrne (2005) considered the influence of the seepage factor by adding the ratio of the inside and outside seepage coefficients of the bucket into the equation. In this paper, the ratio of seepage coefficients inside and outside the bucket is also used to calculate the critical negative pressure under the influence of seepage, and the results are shown in Fig. 14. The comparison of the theoretical results with the experimental critical negative pressures is shown in Fig.22.

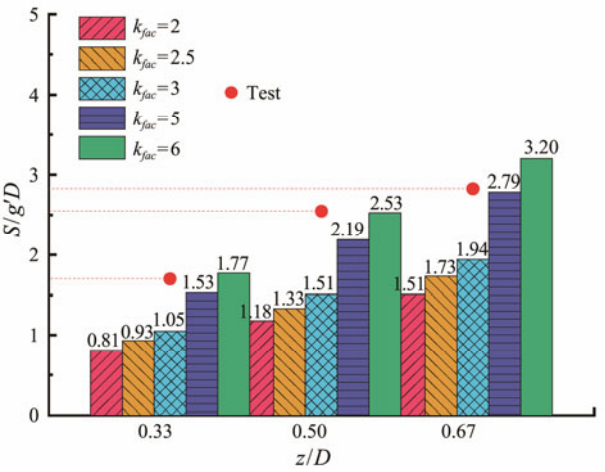

Fig.22 Comparison of theoretical critical negative pressures under different permeability coefficient ratios with the experiment results.

In the Houlsby and Byrne model, the influence of seepage flow on the permeability coefficients inside and outside the bucket is considered. When the ratio of the permeability coefficients inside and outside the bucket is set to 2, 2.5 and 3, the theoretical critical negative pressures increase with the permeability coefficients, but the theoretical values are still about 1.7 times smaller than the test values. When the permeability coefficient ratio is between 5 and 6, the theoretical critical negative pressure values are close to the experimental values.

6 Conclusions

Through the penetrating test and critical negative pressure test for the four-bucket foundation in sand, the movement characteristics and seepage failure characteristics of the foundation when penetrating in sand are discussed, and the applicability of the theoretical formulas for the sinking resistance and critical head is verified. For the negative pressure penetrating process, the Feld theoretical critical negative pressure is used as the upper limit of negative pressure control index, and the penetration resistance calculated by API theory is used as the lower limit of control index to ensure the smooth sinking of the four-tube foundation. Based on the API theoretical model, the prediction of penetration resistance of the four-bucket foundation in sand has a certain degree of credibility.

The foundation sinks fast when the negative pressure is initially loaded. Keep the pressure unchanged, and the foundation sinks slower and slower until a new equilibrium state is reached and the foundation no longer sinks. In order to improve the efficiency in the sinking and penetration process, the negative pressure can only be reasonably increased at a suitable rate.

When the negative pressures in the bucket tubes reach the critical values, the soil will not immediately undergo the seepage failure. After this pressure in the bucket continues for a period of time, the soil will gradually enter the seepage failure state. The external soils of the foundation will pour into the buckets, forming a piping channel, and the negative pressures inside the buckets are rapidly reduced. When the seepage failure occurs, the internal pressures of the buckets reduce to zero.

For the critical water head of the four-bucket foundation in sand, the test critical negative pressure is about 3 times higher than the theoretical critical negative pressure without considering the seepage effect. For the Houlsby and Byrne calculation model, involving the seepage coefficient, the permeability coefficient ratio should be between 5 and 6.

Acknowledgement

The authors would like to acknowledge the support from the National Natural Science Foundation of China (No. 52171274).

References

Achmus, M., Akdag, C., and Thieken, K., 2013. Load-bearing behavior of suction bucket foundations in sand. *Applied Ocean Research*, **43**: 157-165.

American Petroleum Institute, 2014. Geotechnical and foundation design considerations. API RP 2GEO.

Andersen, K., Jostad, H., and Dyvik, R., 2008. Penetration resistance of offshore skirted foundations and anchors in dense sand. *Journal of Geotechnical and Geoenvironmental Engineering*, **134** (1): 106-116.

Barari, A., and Ibsen, L., 2012. Undrained response of bucket foundations to moment loading. *Applied Ocean Research*, **36**: 12-21.

Det Norske Veritas, 2017. Offshore soil mechanics and geotechnical engineering. Offshore Standard DNVGL-RP-C212.

Ding, H., Feng, Z., Zhang, P., Le, C., and Guo, Y., 2020a. Floating performance of a composite bucket foundation with an offshore wind tower during transportation. *Energies*, **13** (4): 882.

Ding, H., Hu, R., Zhang, P., and Le, C., 2020b. Load bearing behaviors of composite bucket foundations for offshore wind turbines on layered soil under combined loading. *Ocean Engineering*, **198**: 106997.

Ding, H., Jia, N., Zhang, P., Le, C., and Liu, Y., 2017. Analysis of penetration test of composite bucket foundations for offshore wind turbines in silty clay. *Journal of Tianjin University*, **50**: 893-899.

Feld, T., 2001. Suction buckets, a new innovative foundation concept, applied to offshore wind turbines. PhD thesis. Aalborg University.

Houlsby, G., and Byrne, B., 2005. Design procedures for installation of suction caissons in sand. *Proceedings of the Institution of Civil Engineers – Geotechnical Engineering*, **158**: 135-144.

Hu, R., Zhang, P., Ding, H., and Le, C., 2018. Numerical analysis of seepage field of bucket foundations for offshore wind turbines. *Ships and Offshore Structures*, **13** (8): 822-834.

Ibsen, L., and Thilsted, C., 2010. Numerical study of piping limits for suction installation of offshore skirted foundations and anchors in layered sand. *Frontiers in Offshore Geotechnics II: Proceedings of the 2nd International Symposium on Frontiers in Offshore Geotechnics*. Perth, 421-426.

Jia, N., Zhang, P., Liu, Y., and Ding, H., 2018. Bearing capacity of composite bucket foundations for offshore wind turbines in silty sand. *Ocean Engineering*, **151**: 1-11.

Kim, J. H., and Kim, D. S., 2019. Soil plug heave induced by suction bucket installation on sand *via* centrifuge model tests. *Marine Georesources & Geotechnology*, **38** (10): 1245-1256.

Lin, S., Fu, D., Zhou, Z., Yan, Y., and Yan, S., 2021. Numerical investigation to the effect of suction-induced seepage on the settlement in the underwater vacuum preloading with prefabricated vertical drains. *Journal of Marine Science and Engineering*, **9** (8): 797.

Sahota, B., and Wilson, Q., 1982. The breakout behavior of suction anchors embedded in submerged sands. *Offshore Technology Conference*. Houston, OTC-4175-MS.

Senders, M., and Randolph, M., 2009. CPT-Based method for the installation of suction caissons in sand. *Journal of Geotechnical and Geoenvironmental Engineering*, **135** (1): 14-25.

Shi, W., Zhang, L. X., Karimirad, M., Michailides, C., Jiang, Z. Y., and Li, X., 2022. Combined effects of aerodynamic and second-order hydrodynamic loads for floating wind turbines at different water depths. *Applied Ocean Research*, **130**: 103416.

Shonberg, A., Harte, M., Aghakouchak, A., Brown, C. S. D., Andrade, M. P., and Liingaard, M. A., 2017. Suction bucket jackets for offshore wind turbines: Applications from *in situ* observations. *Proceeding of TC209 Workshop, 19th International Conference on Soil Mechanics and Geotechnical Engineering*. Seoul, 65-77.

Villalobos, F., Byrne, B., and Houlsby, G., 2010. Model testing of suction caissons in clay subjected to vertical loading. *Applied Ocean Research*, **32**: 414-424.

Wang, X., Zeng, X., and Li, J., 2019. Vertical performance of suction bucket foundation for offshore wind turbines in sand. *Ocean Engineering*, **180**: 40-48.

Wu, Y., Li, D., Zhang, Y., and Chen, F., 2018. Determination of maximum penetration depth of suction caissons in sand. *KSCE Journal of Civil Engineering*, **22**: 2776-2783.

Wu, Y., Zhang, Y., and Li, D., 2020. Solution to critical suction pressure of penetrating suction caissons into clay using limit analysis. *Applied Ocean Research*, **101**: 102264.

Xiao, Z., Fu, D., Zhou, Z., Lu, Y., and Yan, Y., 2019. Effects of strain softening on the penetration resistance of offshore bucket foundation in nonhomogeneous clay. *Ocean Engineering*, **193**: 106594.

Zhang, Y., Shi, W., Li, D. H., Li, X., Duan, Y. F., and Verma, A. S., 2022. A novel framework for modeling floating offshore wind turbines based on the vector form intrinsic finite element (VFIFE) method. *Ocean Engineering*, **262**: 112221.

Zou, M. Y., Chen, M. S., Zhu, L., Li, L., and Zhao, W. H., 2022. A constant parameter time domain model for dynamic modelling of multi-body system with strong hydrodynamic interactions. *Ocean Engineering*, **268**: 113376.

(Edited by Chen Wenwen)